

## Encapsulation of Phthalocyanine Supramolecular Stacks into Virus-like Particles

Melanie Brasch,<sup>†</sup> Andrés de la Escosura,<sup>\*,‡</sup> Yujie Ma,<sup>†</sup> Charlotte Uetrecht,<sup>§</sup> Albert J. R. Heck,<sup>§</sup> Tomás Torres,<sup>‡,||</sup> and Jeroen J. L. M. Cornelissen<sup>\*,†</sup>

<sup>†</sup>Laboratory for Biomolecular Nanotechnology, MESA+ Institute, University of Twente, P.O. Box 207, 7500 AE Enschede, The Netherlands

<sup>‡</sup>Organic Chemistry Department, Universidad Autónoma de Madrid, 28049 Cantoblanco, Spain

<sup>§</sup>Biomolecular Mass Spectrometry and Proteomics Group, Utrecht Institute of Pharmaceutical Science and Bijvoet Centre, Utrecht University and Netherlands Proteomics Centre, 3508 TC Utrecht, The Netherlands

<sup>||</sup>IMDEA-Nanociencia, Facultad de Ciencias, Ciudad Universitaria de Cantoblanco, 28049 Madrid, Spain

**S** Supporting Information

**ABSTRACT:** We report herein the encapsulation of a water-soluble phthalocyanine (Pc) into virus-like particles (VLPs) of two different sizes, depending on the conditions. At neutral pH, the cooperative encapsulation/templated assembly of the particles induces the formation of Pc stacks instead of Pc dimers, due to an increased confinement concentration. The Pc-containing VLPs may potentially be used as photosensitizer/vehicle systems for biomedical applications such as photodynamic therapy.

Light-absorbing organic molecules such as porphyrins (Por's) and phthalocyanines (Pc's) are widely used building blocks in materials science and nanotechnology.<sup>1,2</sup> Pc's, in particular, are very robust and versatile chromophores with numerous applications in medicine, photonics, electronics, and energy conversion.<sup>3–7</sup> Pc's tend to aggregate and form stacks through  $\pi$ – $\pi$  aromatic interactions. Controlling the size and structure of such stacks represents an efficient way to determine the properties of these macrocycles. In this respect, viruses have been proposed as well-defined and monodisperse platforms for the organization of chemical entities both in their inner cavities and on their exterior surfaces.<sup>8–14</sup> The protein scaffold of rod-like viruses, such as the bacteriophage M13<sup>15,16</sup> and the tobacco mosaic virus (TMV),<sup>17</sup> or icosahedral ones, such as the hepatitis B virus (HBV)<sup>18</sup> and the bacteriophage MS2,<sup>19</sup> have been decorated with Por's. In all these cases, the viral proteins required modification by molecular biology techniques for the subsequent covalent<sup>16–19</sup> or non-covalent<sup>15</sup> interaction with the Por moieties. Herein, we describe a very simple method for the encapsulation of a water-soluble zinc Pc (ZnPc) into virus-like particles (VLPs), in which the chromophore and the native virus protein are simply co-incubated in solution (Figure 1). Interestingly, capsids of two different sizes can be obtained, depending on the pH. The superior optical and electronic properties of Pc's together with the biocompatible nature of the nanocontainer makes our approach very appealing for biomedical applications.

The coat protein (CP) of the cowpea chlorotic mottle virus (CCMV) has shown its ability for inducing the self-assembly of

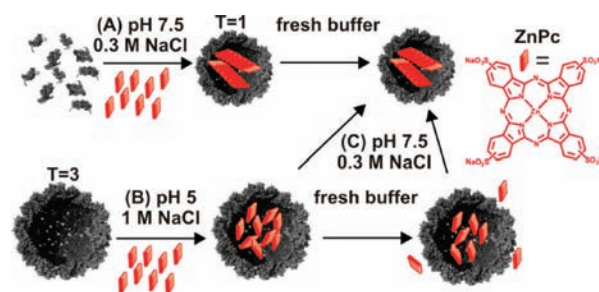


**Figure 1.** Schematic representation of the encapsulation of Pc stacks into CCMV VLPs. The length and arrangement of the stacks within the capsids in the cartoon are tentative.

VLPs.<sup>13</sup> CCMV is a plant virus with inner and outer diameters of 18 and 28 nm, respectively.<sup>20,21</sup> The interior of the capsid is positively charged. At neutral pH and high ionic strength, the capsid disassembles into 90 identical CP dimers. After removal of the viral RNA, capsids of the same size and geometry as the native virus ( $T = 3$ )<sup>22</sup> can be reassembled if the pH is dropped back to 5, while smaller capsids ( $T = 1$ )<sup>23</sup> are formed at pH 7.5 if polyanionic species are present in the solution.<sup>24,25</sup>

The aggregation behavior of metal Pc tetrasulfonic acid salts has been well characterized in the literature.<sup>26</sup> At low concentrations (i.e.,  $10^{-4}$ – $10^{-7}$  M), these Pc derivatives normally form dimers, with their absorption maximum centered at  $\lambda \approx 635$  nm, while monomeric species absorb at  $\lambda = 680$ – $690$  nm (Supporting Information (SI), Figures S2 and S3A). The blue-shift of the ZnPc Q-band indicates a H type of aggregation, with contiguous ZnPc molecules in a co-facial arrangement.<sup>2</sup> For higher concentrations of ZnPc, its aggregation has also been evaluated by dynamic light scattering (DLS) (SI, Figure S4), revealing that large aggregates are formed at concentrations higher than 1 mM.

The encapsulation of ZnPc inside the VLPs was accomplished by two different routes. First, ZnPc and CP solutions (with final concentrations of  $[\text{ZnPc}] = 1$  mM and  $[\text{CP}] = 0.2$  mM) in Tris-HCl buffer (50 mM, 0.3 M NaCl, 1 mM DTT, pH 7.5) were

**Received:** November 30, 2010

**Published:** April 20, 2011

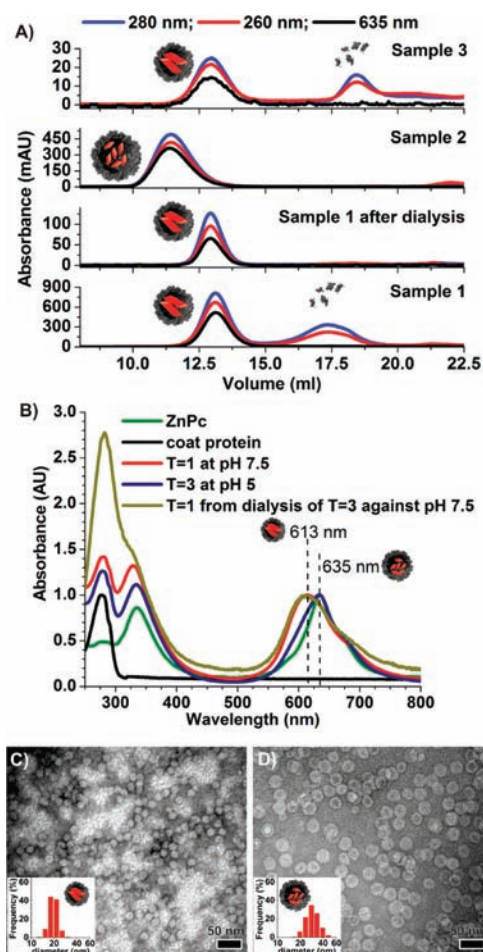


**Figure 2.** (A) FPLC chromatograms of Samples 1, 2, and 3. (B) Normalized UV-vis spectra of ZnPc, CP, and FPLC fractions from Samples 1, 2, and 3. (C) TEM micrograph and DLS size distribution diagram (inset) of Pc-containing  $T = 1$  particles from the FPLC fraction of Sample 1. (D) TEM micrograph and DLS size distribution diagram (inset) of ZnPc-containing  $T = 3$  particles from the FPLC fraction of Sample 2. In (C) and (D), scale bar = 50 nm.

mixed and incubated for 1 h at 4 °C (Figure 1A). Analysis of the sample by fast protein liquid chromatography (FPLC) showed peaks eluting at 12.8 and 17.5 mL (Figure 2A, Sample 1). It can be inferred, by comparison with the FPLC chromatogram of a solution lacking the ZnPc (SI, Figure S5), that the second peak corresponds to CP dimers. The peak at 12.8 mL, on the other hand, can be ascribed to  $T = 1$  particles, according to the transmission electron microscopy (TEM) micrographs obtained from the corresponding FPLC fraction (Figure 2C). On the basis of integration of the FPLC peaks, we estimate that 71% of the starting CP material was used for the encapsulation process, forming  $T = 1$  particles. The particles were purified by dialysis against fresh Tris-HCl buffer. The strong absorption of the FPLC peak at 635 nm clearly indicates that the particles are loaded with ZnPc (Figure 2A, Sample 1 after dialysis). Analysis of the TEM images from this sample yielded  $T = 1$  capsids with an average diameter of  $19 \pm 5$  nm. DLS measurements gave similar results (Figure 2C, inset).

Interestingly, the UV-vis spectrum of the peak fraction shows a blue-shift of the ZnPc Q-band compared to the non-encapsulated ZnPc, from 635 to 613 nm (Figure 2B). The average number of

ZnPc molecules per particle and their concentration inside the capsids were estimated by using calibration lines constructed from the absorption values of ZnPc and the CP (SI, Figure S3B). The concentration of ZnPc incorporated within the capsids was estimated to be 0.12 M, which corresponds to two ZnPc's per CP subunit (i.e., 120 ZnPc molecules in each capsid). Such estimation by UV-vis spectroscopy is, however, quite rough, due to the hypsochromic shift observed for the ZnPc absorption.

To determine the number of ZnPc molecules per capsid more accurately, the sample was subjected to native electrospray ionization mass spectrometry (ESI-MS). An average number of  $192 \pm 20$  ZnPc molecules per particle was obtained (SI, Figure S6).<sup>27,28</sup> Such a high local concentration, likely resulting from the strong electrostatic interaction between negative ZnPc dimers and the positive CP N-terminus during the encapsulation process, explains the stronger aggregation of ZnPc compared to what is expected for its overall concentration in Sample 1. In fact, there was no diffusion of Pc molecules out of the capsids during the dialysis purification step, as indicated by the absence of changes in the UV-vis absorption of the FPLC fraction (SI, Figure S5).

For the second encapsulation route, a mixture of ZnPc and empty  $T = 3$  capsids (with final concentrations of [ZnPc] = 1 mM and [CP] = 0.23 mM) was incubated in sodium acetate buffer (50 mM, 1 M NaCl, 1 mM NaN<sub>3</sub>, pH 5) for 1 h at 4 °C. Under these conditions, ZnPc needs to diffuse through the capsid pores to be encapsulated. The FPLC chromatogram obtained from the mixture showed a clear peak eluting at 11 mL, with an intense absorption at 635 nm (Figure 2A, Sample 2). TEM analysis of the FPLC fraction (Figure 2D) and comparison of the chromatogram with that of empty capsids (SI, Figure S5) indicated that this peak corresponds to  $T = 3$  particles. The UV-vis spectrum of the FPLC fraction shows the absorption maximum centered around 635 nm (Figure 2B). It thus seems that  $T = 3$  capsids do not force the ZnPc to aggregate further than forming dimers. Moreover, the FPLC chromatogram of Sample 2 after dialysis against fresh acetate buffer shows that ZnPc molecules substantially diffuse out of the capsids (SI, Figure S3), decreasing the local concentration of ZnPc from 57 to 38 mM (estimated by UV-vis spectroscopy). The leakage of ZnPc molecules from  $T = 3$  capsids was confirmed when free ZnPc, which does not elute under buffering conditions, was eluted in an extra run with pure water as the eluent (SI, Figure S7).

The ZnPc-containing  $T = 3$  particles are not stable at neutral pH. Dialysis of Sample 2 against Tris-HCl buffer (50 mM, 0.3 M NaCl, 1 mM DTT, pH 7.5) transformed the  $T = 3$  into  $T = 1$  particles (61%) and free CP (39%), as revealed by FPLC (Figure 2A, Sample 3) and TEM. In this process, the absorption maximum of the Pc stacks decreases again to 613 nm (Figure 2B). These findings are in agreement with the high robustness observed for the ZnPc-containing  $T = 1$  capsids. For instance, they stay intact after dialysis against Milli-Q water (SI, Figure S8). Moreover, an additional dialysis back to pH 5 sodium acetate buffer does not recover the  $T = 3$  capsids (SI, Figure S9).

The stronger aggregation of ZnPc inside the  $T = 1$  capsids, which cannot even be disrupted by the addition of water-soluble pyridine derivatives (e.g., 10% picolinic acid; SI, Figure S8),<sup>29</sup> is likely related to the different driving force that directs the assembly depending on the pH.  $T = 3$  capsids are thermodynamically stable at pH 5 and do not need a template for their assembly. In contrast, electrostatic interactions between the CP and the cargo are dominant at pH 7.5.<sup>30</sup> The ZnPc stacks are then needed to template the formation of  $T = 1$  capsids and cannot



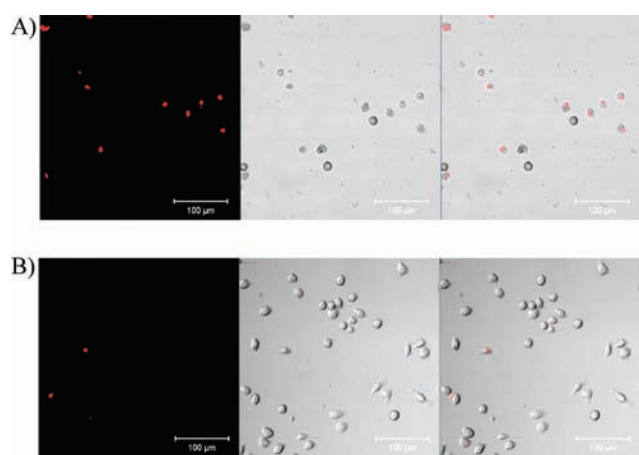


**Figure 3.** Micrographs obtained when a culture of RAW 264.7 macrophage cells was irradiated with a mercury lamp (excitation BP wavelengths of 620/60 nm) for 20 min, (A) in the presence of ZnPc-loaded  $T = 1$  capsids (high magnification; for low magnification see SI, Figure S10A) and (B) in their absence (high magnification; for low magnification see SI, Figure S10D). Dead cells were stained with PI and they appear colored in red in the fluorescence image. Left, fluorescence images (excitation at 543 nm, emission recorded with a LP 560 filter); middle, transmission images; right, overlap of the other two images.

diffuse out of the evidently very stable protein cage. Such a cooperative encapsulation/templated assembly process strongly promotes the aggregation of ZnPc at neutral pH.

Pc's are promising candidates as photosensitizers for photodynamic therapy (PDT) of neoplastic and non-neoplastic diseases.<sup>1</sup> An important requirement in this respect is the transport of the Pc to the target tissue. Although the tetrasulfonated ZnPc is not an ideal photosensitizer, because aggregation partially quenches the Pc excited states, current efforts are underway to evaluate the PDT activity of ZnPc-containing CCMV capsids. Preliminary experiments have shown that  $T = 3$  and  $T = 1$  capsids loaded with ZnPc were incorporated by macrophage cells.<sup>31</sup> Subsequent irradiation for 20 min with a mercury lamp, at excitation wavelengths in the range of 620–660 nm, provoked the almost complete death (92–95%, SI, Table S1) of cells in the illuminated area (Figure 3A and SI, Figure S10A,B), whereas in the non-illuminated area cells survive. The presence of dead cells was evaluated by staining with propidium iodide (PI), which intercalates into double-stranded nucleic acids. PI is excluded by viable cells but can penetrate the cell membrane of dying or dead cells. Dead cells are thus identified in the micrographs as they appear red in the fluorescence images. The ZnPc induces a similar PDT effect (92%, SI, Table S1) in the absence of CP (SI, Figure S10C). In contrast, when irradiation took place in the absence of ZnPc and the CP, almost no dead cells (5%, Table S1) could be observed (Figure 3B and SI, Figure S10D).

The suitability of ZnPc-loaded CCMV  $T = 1$  particles to induce cell death upon cellular uptake and subsequent irradiation has been proved by these experiments. An experimental confirmation of whether encapsulated or free ZnPc is the species responsible for cellular death unfortunately could not be obtained. The encapsulation of ZnPc presents, however, plenty of potential benefits for PDT *in vivo*. The photosensitizer biocompatibility may be improved during its transport through the organism. Moreover, our strategy could facilitate cellular targeting

and would certainly provide an increased local concentration. Future implementations, such as the encapsulation of non-aggregated Pc derivatives and the capsid functionalization with target-selective biocompatible polymers, are envisioned. Understanding how these factors would affect the assembly properties of the CP and the efficacy of the PDT response will be of fundamental importance in the route toward an efficient photosensitizer/vehicle system. Interestingly, the analogous copper derivative of ZnPc (tetrasulfonated CuPc) has been used to target G-quadruplexes and to selectively inhibit the elongation of telomers (i.e., one of the main causes of cell canceration) in the presence of dsDNA.<sup>32</sup> These Pc-containing VLPs may therefore be potentially useful for the inhibition of telomerase activity.

Our data furthermore show that the assembly of artificially loaded icosahedral protein cages is a complex process, with a delicate interplay between capsid protein and cargo. On one hand the formation of  $T = 1$  particles at neutral pH is due to the presence of a negatively charged template. On the other hand, the high effective concentration resulting from the dye confinement leads to larger ZnPc aggregates, which in turn might be better templates. This cooperative association between protein assembly and ZnPc aggregation yields, in the end, a stable Pc-loaded protein nanocontainer.

## ■ ASSOCIATED CONTENT

**S Supporting Information.** Materials and methods; characterization of **1** and its aggregation behavior; complete FPLC, MS, and UV–vis study of the ZnPc-containing VLPs; and phototoxicity studies in cells. This material is available free of charge via the Internet at <http://pubs.acs.org>.

## ■ AUTHOR INFORMATION

### Corresponding Author

J.J.L.M.Cornelissen@utwente.nl; andres.delaescosura@uam.es

## ■ ACKNOWLEDGMENT

The authors acknowledge financial support by the Spanish MICINN, MEC [CTQ2008-00418/BQU (T.T., A.E.) and CONSOLIDER-INGENIO 2010, CDS2007-00010, Nanociencia Molecular (T.T., A.E.)] and CAM [MADRISOLAR-2, S2009/PPQ/1533 (T.T., A.E.)], The Chemical Council of The Netherlands National Science Foundation (NWO-CW), the European Science Foundation (ESF), and The Netherlands Royal Academy for Arts and Sciences (KNAW).

## ■ REFERENCES

- (1) de la Torre, G.; Claessens, C. G.; Torres, T. *Chem. Commun.* **2007**, 2000–2015.
- (2) Kadish, K. M.; Smith, K. M.; Guillard, R. *Handbook of Porphyrin Science*; World Scientific: Singapore, 2010.
- (3) O'Flaherty, S. M.; Hold, S. V.; Cook, M. J.; Torres, T.; Chen, Y.; Hanack, M.; Blau, W. J. *Adv. Mater.* **2003**, *15*, 19–32.
- (4) Kobayashi, N.; Leznoff, C. C. *J. Porphyrins Phthalocyanines* **2004**, *8*, 1015–1019.
- (5) Bottari, G.; Olea, D.; Gomez-Navarro, C.; Zamora, F.; Gomez-Herrero, J.; Torres, T. *Angew. Chem. Int. Ed.* **2008**, *47*, 2026–2031.
- (6) Jiang, J. Z.; Ng, D. K. P. *Acc. Chem. Res.* **2009**, *42*, 79–88.
- (7) Bottari, G.; de la Torre, G.; Guldi, D. M.; Torres, T. *Chem. Rev.* **2010**, *110*, 6768–6816.

- (8) Wang, Q.; Lin, T. W.; Tang, L.; Johnson, J. E.; Finn, M. G. *Angew. Chem. Int. Ed.* **2002**, *41*, 459–462.
- (9) Douglas, T.; Young, M. *Science* **2006**, *312*, 873–875.
- (10) Nam, K. T.; Kim, D. W.; Yoo, P. J.; Chiang, C. Y.; Meethong, N.; Hammond, P. T.; Chiang, Y. M.; Belcher, A. M. *Science* **2006**, *312*, 885–888.
- (11) Fischlechner, M.; Donath, E. *Angew. Chem. Int. Ed.* **2007**, *46*, 3184–3193.
- (12) Rotello, V. M. *J. Mater. Chem.* **2008**, *18*, 3739–3740.
- (13) de la Escosura, A.; Nolte, R. J. M.; Cornelissen, J. J. L. M. *J. Mater. Chem.* **2009**, *19*, 2274–2278.
- (14) Kostiainen, M. A.; Kasyutich, O.; Cornelissen, J. J. L. M.; Nolte, R. J. M. *Nature Chem.* **2010**, *2*, 394–399.
- (15) Scolaro, L. M.; Castriciano, M. A.; Romeo, A.; Micali, N.; Angelini, N.; Lo Passo, C.; Felici, F. *J. Am. Chem. Soc.* **2006**, *128*, 7446–7447.
- (16) Nam, Y. S.; Shin, T.; Park, H.; Magyar, A. P.; Choi, K.; Fantner, G.; Nelson, K. A.; Belcher, A. M. *J. Am. Chem. Soc.* **2010**, *132*, 1462–1463.
- (17) Endo, M.; Fujitsuka, M.; Majima, T. *Chem. Eur. J.* **2007**, *13*, 8660–8666.
- (18) Prasuhn, D. E.; Kuzelka, J.; Strable, E.; Udit, A. K.; Cho, S. H.; Lander, G. C.; Quispe, J. D.; Diers, J. R.; Bocian, D. F.; Potter, C.; Carragher, B.; Finn, M. G. *Chem. Biol.* **2008**, *15*, 513–519.
- (19) Stephanopoulos, N.; Carrico, Z. M.; Francis, M. B. *Angew. Chem. Int. Ed.* **2009**, *48*, 9498–9502.
- (20) Speir, J. A.; Munshi, S.; Wang, G. J.; Baker, T. S.; Johnson, J. E. *Structure* **1995**, *3*, 63–78.
- (21) Johnson, J. E.; Speir, J. A. *J. Mol. Biol.* **1997**, *269*, 665–675.
- (22)  $T$  represents the triangulation number, a geometrical parameter that characterizes icosahedral structures.  $T = 1$  and  $T = 3$  capsids are formed by 60 and 180 CP subunits, respectively.
- (23) Sikkema, F. D.; Comellas-Aragones, M.; Fokkink, R. G.; Verduin, B. J. M.; Cornelissen, J. J. L. M.; Nolte, R. J. M. *Org. Biomol. Chem.* **2007**, *5*, 54–57.
- (24) Tang, J. H.; Johnson, J. M.; Dryden, K. A.; Young, M. J.; Zlotnick, A.; Johnson, J. E. *J. Struct. Biol.* **2006**, *154*, 59–67.
- (25) Lavelle, L.; Gingery, M.; Phillips, M.; Gelbart, W. M.; Knobler, C. M.; Cadena-Nava, R. D.; Vega-Acosta, J. R.; Pinedo-Torres, L. A.; Ruiz-Garcia, J. *J. Phys. Chem. B* **2009**, *113*, 3813–3819.
- (26) Nyokong, T. *Coord. Chem. Rev.* **2007**, *251*, 1707–1722.
- (27) The number of ZnPc molecules per capsid could be up to  $\sim 20$  molecules lower, as estimated from the peak width in MS.
- (28) Heck, A. J. R. *Nature Methods* **2008**, *5*, 927–933.
- (29) The addition of pyridine derivatives generally disrupts the aggregation of ZnPc's by coordination to the zinc central atom of the macrocycle.
- (30) Burns, K.; Mukherjee, S.; Keef, T.; Johnson, J. M.; Zlotnick, A. *Biomacromolecules* **2010**, *11*, 439–442.
- (31) However,  $T = 3$  particles are not considered so suitable as ZnPc carriers as their  $T = 1$  counterparts, since they have been shown to rearrange and release part of the encapsulated ZnPc molecules into the medium (see previous paragraphs).
- (32) Yaku, H.; Murashima, T.; Miyoshi, D.; Sugimoto, N. *Chem. Commun.* **2010**, *46*, 5740–5742.